Development of social feedback processing and responses in childhood: an fMRI test-replication design in two age cohorts

Simone Dobbelaar,[iD][1,2,3,4] Michelle Achterberg,[1,2,3,4] Lina van Drunen,[1,2,3,4] Anna C.K. van Duijvenvoorde,[1,2,3]
Marinus H. van IJzendoorn,[1,4,5] and Eveline A. Crone[1,2,3,4]

[1]Leiden Consortium on Individual Development, Leiden University, Leiden 2333 AK, The Netherlands
[2]Developmental and Educational Psychology, Faculty of Social and Behavioural Sciences, Leiden University, Leiden 2333 AK, The Netherlands
[3]Leiden Institute for Brain and Cognition, Leiden University, Leiden 2300 RC, The Netherlands
[4]Department of Psychology, Education and Child Studies, Erasmus School of Social and Behavioural Sciences, Erasmus University Rotterdam, Rotterdam 3000 DR, The Netherlands
[5]Research Department of Clinical, Education and Health Psychology, University College London, London WC1E 6BT, UK
Correspondence should be addressed to Simone Dobbelaar, Developmental and Educational Psychology, Leiden University, Wassenaarseweg 52, Leiden 2333 AK, the Netherlands. E-mail: s.dobbelaar@fsw.leidenuniv.nl.

Abstract

This study investigated behavioral and neural correlates underlying social feedback processing and subsequent aggressive behaviors in childhood in two age cohorts (test sample: $n = 509/n = 385$ and replication sample: $n = 354/n = 195$, 7–9 years old). Using a previously validated Social Network Aggression Task, we showed that negative social feedback resulted in most behavioral aggression, followed by less aggression after neutral and least aggression after positive feedback. Receiving positive and negative social feedback was associated with increased activity in the insula, medial prefrontal cortex and ventrolateral prefrontal cortex. Responding to feedback was associated with additional activation in the dorsolateral prefrontal cortex (DLPFC) following positive feedback. This DLPFC activation correlated negatively with aggression. Furthermore, age analyses showed that older children showed larger reductions in aggression following positive feedback and more neural activation in the DLPFC when responding to positive feedback compared to younger children. To assess the robustness of our results, we examined these processes in two independent behavioral/functional magnetic resonance imaging samples using equivalence testing, thereby contributing to replicable reports. Together, these findings demonstrate an important role of social saliency and regulatory processes where regulation of aggression rapidly develops between the ages of 7 and 9 years.

Key words: social feedback processing; aggression regulation; fMRI; childhood; replication

Introduction

Middle childhood, the developmental phase from ~7 to 10 years of age (DeFries *et al.*, 1994), is an important period marked by rapid developmental changes in social competencies needed for developing adaptive social relations. For example, children more often experience and respond to social evaluations of peers. Prior research in adults and children showed that social rejection can lead to aggressive, retaliatory responses (Chester *et al.*, 2014; Achterberg *et al.*, 2017). An unanswered question, however, is how feedback processing and subsequent aggressive responses develop during childhood and which neural processes are involved. This study examined behavioral and neural responses to social feedback and subsequent aggression in middle childhood, using a test-replication design to optimize reliable and robust analyses.

Neural correlates of social feedback processing

In prior studies, functional magnetic resonance imaging (fMRI) was used to specifically focus on neural activity when participants received social feedback (Gunther Moor *et al.*, 2010; Guyer *et al.*, 2012; Achterberg *et al.*, 2017, 2018). The medial prefrontal cortex (MPFC), anterior insula (AI) and anterior cingulate cortex (ACC) showed enhanced activation during both positive and negative feedback compared to neutral feedback in prior studies in adults (Achterberg *et al.*, 2016) and children (Achterberg *et al.*, 2017, 2018, 2020). These regions have often been identified as regions involved in not only social cognition tasks, such as social evaluation and self-other referential processing (Blakemore and Mills, 2014; Apps *et al.*, 2016; Yoon *et al.*, 2018; Crone *et al.*, 2020), but also in nonsocial tasks, such as cognitive control, attentional processes and memory (e.g. Menon and Uddin, 2010; Euston *et al.*,

2012). In social feedback paradigms, the MPFC, AI and ACC might be specifically responsive to feedback that is salient (both positive and negative). Activation related to positive feedback has been reported in the ventral striatum, dorsolateral prefrontal cortex (DLPFC) and supplementary motor area (SMA), in adults (Achterberg *et al.*, 2016), children and adolescents (Gunther Moor *et al.*, 2010; Guyer *et al.*, 2012; Achterberg *et al.*, 2017, 2018). In contrast, negative feedback has been associated with activity in the superior MPFC (Achterberg *et al.*, 2016, 2018), although it is not consistently observed across studies (Guyer *et al.*, 2012). During negative feedback processing, enhanced DLPFC activation has been associated with subsequent aggression reduction (Riva *et al.*, 2015; Achterberg *et al.*, 2016, 2018). Given that replicability of fMRI findings in childhood is still relatively understudied and task-based fMRI shows low test–retest reliability (Elliott *et al.*, 2020), the first aim of this study was to replicate previously observed neural responses to social feedback and the relation to individual differences in aggression in a large sample of children aged 7–9 years (Open Science Collaboration, 2015; Schmidt, 2016; van IJzendoorn and Bakermans-Kranenburg, 2021).

Neural correlates of responding to social feedback

The Social Network Aggression Task (SNAT; Achterberg *et al.*, 2016) has been developed to study the effects of receiving social feedback on subsequent aggressive responses. In this task, participants first received social peer feedback and were subsequently instructed to respond by sending a noise blast toward the peer giving the feedback. Negative feedback consistently resulted in the longest noise blasts compared to positive and neutral feedback, in adults and children (Chester *et al.*, 2014; Achterberg *et al.*, 2016, 2017, 2018). Supplementary Table S1 shows an overview of previous findings in studies using the SNAT.

A still unexplored question of this study is which neural processes underlie these responses to social feedback in childhood. In adults, studies on neural activity during aggression following negative feedback show mixed results. For example, aggression following high (*vs* low) provocation, i.e. reactive aggression, has been associated with increased activation in the insula, ACC, MPFC, DLPFC, ventrolateral prefrontal cortex (VLPFC) (Krämer *et al.*, 2007; Lotze *et al.*, 2007; Dambacher *et al.*, 2015; Repple *et al.*, 2017), ventral striatum (Buades-Rotger *et al.*, 2016; Chester and DeWall, 2016) and orbitofrontal cortex (OFC; Repple *et al.*, 2017). On the other hand, increased aggression or punishment of unfair offers in an Ultimatum Game has also been related to decreased OFC and ventral MPFC activation (Mehta and Beer, 2010; White *et al.*, 2014; Beyer *et al.*, 2015; Gilam *et al.*, 2015). Additionally, to our knowledge, only two prior studies investigated neural activation during forced aggressive responses following positive feedback. These studies reported increased activation in the DLPFC during responses to positive compared to negative feedback in the SNAT (van de Groep *et al.*, 2021, 2022). Therefore, the second aim of our study was to investigate neural activity during responses to positive, neutral and negative social feedback.

In the SNAT, where participants are instructed to always send a noise blast, increased DLPFC activation following positive feedback (van de Groep *et al.*, 2021) may possibly reflect inhibitory processes. DLPFC activation has previously been related to impulse control in nonsocial contexts (Durston *et al.*, 2002; Blasi *et al.*, 2006), and we hypothesize that it might play a similar role when responding to social feedback. Therefore, we additionally aimed to study whether individual differences in DLPFC activation following positive (*vs* negative) feedback were related to decreased aggressive responses following positive feedback.

The current study

The current study tested the two processes of feedback processing and responding in the Leiden Consortium on Individual Development (L-CID), which consists of two independent age cohorts with overlapping time points in middle childhood (Crone *et al.*, 2020), allowing for direct replication of our analyses. The experimental SNAT was used to measure neural activation on two events: the social feedback event, when participants received social feedback, and the noise blast event, when participants responded to social feedback by sending a noise blast.

Our first aim (i) was to replicate previously reported valence effects on neural activity during social feedback processing in the AI, MPFC, VLPFC and DLPFC (Achterberg *et al.*, 2020) and related brain–behavior correlations. We hypothesized that DLPFC activation following rejection was related to lower levels of aggression following negative feedback (Achterberg *et al.*, 2018, 2020).

Our second novel aim (ii) was (a) to investigate valence effects on neural activity during responses to social feedback and (b) to test whether individual differences in neural activity were meaningfully related to behavioral aggression. We expected that more DLPFC activation following positive feedback relative to negative feedback would be related to decreased aggressive responses following positive feedback.

Finally, we performed two exploratory analyses (iii). During childhood, the cognitive processes that are important for controlling behavior are still developing (Crone and Steinbeis, 2017). These developmental changes might already be noticeable during the course of middle childhood since this period is marked by a rapid development in regulatory skills (Zelazo and Carlson, 2012; Achterberg *et al.*, 2020). Therefore, we (a) explored age differences in aggression regulation between 7- and 9-year olds to investigate how feedback processing and subsequent aggression develop during childhood. Additionally, to further explore which children might be most prone to aggression following negative feedback, we (b) tested whether parental reported inhibitory control moderated the relation between activation in the affective salience network (AI and MPFC) during feedback and behavioral aggression, such that increased neural sensitivity to social feedback would be related to more reactive aggression only for children with low levels of inhibitory control (Chester *et al.*, 2014).

Methods
Participants

This study was part of the cohort sequential longitudinal twin study 'L-CID' (Euser *et al.*, 2016; Crone *et al.*, 2020). Children in the early childhood cohort (ECC) were followed from 3 to 9 years of age, whereas children in the middle childhood cohort (MCC) were followed from 7 to 13 years (Crone *et al.*, 2020). The present study focused on the first visit of the MCC (test sample) and the fifth visit of the ECC (replication sample), which were lab visits including MRI scans. The overlap in age (7–9 years old) between cohorts allowed for a replication within the same study and for replication of effects that were previously reported by Achterberg *et al.* (2018, 2020) on the MCC data.

In the MCC, data were collected in 2015–16. Data and characteristics of the test sample were previously reported in Achterberg *et al.* (2018). Our behavioral test sample consisted of 509 participants (mean age: 7.95 ± 0.67 years, 51% girls). In total, 124 participants were excluded from MRI analyses (Supplementary Figure S1), resulting in an MRI test sample of 385 participants (mean age: 7.99 ± 0.68 years, 53% girls).

Table 1. Demographic characteristics

	Test sample (MCC)		Replication sample (ECC)	
	Behavioral	**MRI**	**Behavioral**	**MRI**
N	509	385	354	195
Girls (%)	50.9	53.0	53.1	57.4
Age (s.d.)	7.95 (0.67)	7.99 (0.68)	8.00 (0.62)	8.08 (0.62)
Age range	7.02–9.68	7.02–9.68	6.93–9.62	7.02–9.49
Left-handed (%)	12.8	12.2	13.4	12.3
IQ (s.d.)	103.62 (11.77)	104.03 (11.84)	103.24 (10.69)	103.21 (10.74)
IQ range	72.50–137.50	72.50–137.50	75.0–130.0	77.50–130.0
Caucasian (%)	91	93	92	95
SES low–middle–high (%)	9–45–46	8–43–49	5–35–60	2–33–65

Note. SES = socioeconomic status, based on parental education at T1.

In the ECC, data were collected in 2019. Our behavioral replication sample consisted of 354 participants (mean age: 8.00 ± 0.62 years, 53.1% girls). In total, 159 participants were excluded from MRI analyses (Supplementary Figure S1), resulting in an MRI replication sample of 195 participants (mean age: 8.08 ± 0.62 years, 57.4% girls). Sample characteristics are presented in Table 1. Prior to the first visit, informed consent was obtained from both parents. The study was approved by the Dutch Central Committee on Research Involving Human Subjects (CCMO).

Measures

Social Network Aggression Task

Feedback effects and subsequent aggressive responses were measured using the SNAT, which has been validated as a reliable measure of aggression following social feedback (Achterberg *et al.*, 2016, 2017). Participants filled out a personal profile at home and sent this back a week before the lab visit. During the lab visit, participants received feedback from peers on whether they liked the answers on their profiles. This feedback could be positive (a green thumb up), neutral (a gray circle) or negative (a red thumb down). Subsequently, participants had to imagine sending a noise blast toward the peer who had given the feedback by pressing a button with their right index finger. They could decide the intensity of the noise blast by pressing the button for a longer duration (Figure 1A), which was used as a measure of behavioral aggression. Participants were specifically instructed to imagine sending the noise blast to reduce the amount of deception used in the task. Participants did not know that peers in the tasks were not real but were morphed photographs from an existing database. Each photograph was presented with positive, neutral or negative feedback. The order of trials was pseudo-randomized.

The SNAT consisted of 60 trials (three blocks of 20 trials) in the test sample. In the replication sample, we shortened the MRI session, based on findings that scan quality decreases with the increasing length of the scanning procedure (Achterberg and van der Meulen, 2019). Since we found comparable main effects in the MCC data when analyzing two *vs* three blocks of the SNAT, we chose to include 40 trials (two blocks of 20 trials) in the replication sample.

Inhibitory control (Temperament in Middle Childhood Questionnaire)

To measure inhibitory control, the subscale Inhibitory Control of the parental reported version of the Temperament in Middle Childhood Questionnaire was used (Simonds *et al.*, 2007). The primary caregiver, who spent the most time with the children

at the start of the study, completed the questionnaire for both twin children separately. This subscale consisted of eight questions (e.g. 'My child can stop him/herself from doing things too quickly') that were answered on a five-point scale (1 = 'extremely untrue', 5 = 'extremely true'). Cronbach's alpha was 0.67. A mean score over the seven items was computed, such that higher scores indicate more inhibitory control.

MRI data acquisition

MRI scans were acquired on a Philips Ingenia 3.0 Tesla MR system, using a standard whole-head coil. Participants from both samples were scanned using the same MRI scanner. Foam inserts were added within the head coil to minimize head motion. Participants viewed the SNAT on a screen that was placed behind the scanner and could be viewed through a mirror on the head coil. Functional MRI scans were collected using T2*-weighted echo-planar imaging (EPI). The first two volumes were discarded to allow for equilibration of T1 saturation effects [field of view (FOV) = 220 (anterior–posterior, a–p) × 220 (right–left, r–l) × 111.65 (foot–head, f–h) mm; repetition time (TR) = 2.2 s, echo time (TE) = 30 ms; flip angle (FA) = 80°; sequential acquisition; 37 slices; voxel size = 2.75 × 2.75 × 2.75]. In the test sample, the SNAT consisted of three blocks (block 1: 148 volumes, block 2: 142 volumes and block 3: 141 volumes; Achterberg *et al.*, 2018). In the replication sample, the SNAT consisted of two blocks (block 1: 148 volumes and block 2: 142 volumes). The modification between the two samples was introduced to decrease the total scan time (Achterberg and van der Meulen, 2019). In between blocks, scanning was paused to give the participant a small break. Additionally, a high-resolution 3D T1 scan was collected as anatomical reference [FOV = 224 (a–p) × 177 (r–l) × 168 (f–h) mm; TR = 9.72 ms; TE = 4.95 ms; FA = 8°; 140 slices; voxel size = 0.875 × 0.875 × 0.875 mm].

MRI data analyses

fMRI preprocessing

fMRI data were analyzed using Statistical Parametric Mapping software (SPM, Wellcome Department of Cognitive Neurology, London). We used SPM8 for consistency with the previously published study. First, images were corrected for slice timing acquisition and rigid body motion. Functional volumes were spatially normalized to T1 templates using 12-parameter affine transform mapping and nonlinear transformation involving cosine basis functions. Templates were based on the Montreal Neurological Institute (MNI) 305 stereotaxic space (Cocosco *et al.*, 1997). Due to missing 3D T1 data, data of five participants in the test sample were normalized to an EPI template. Volumes
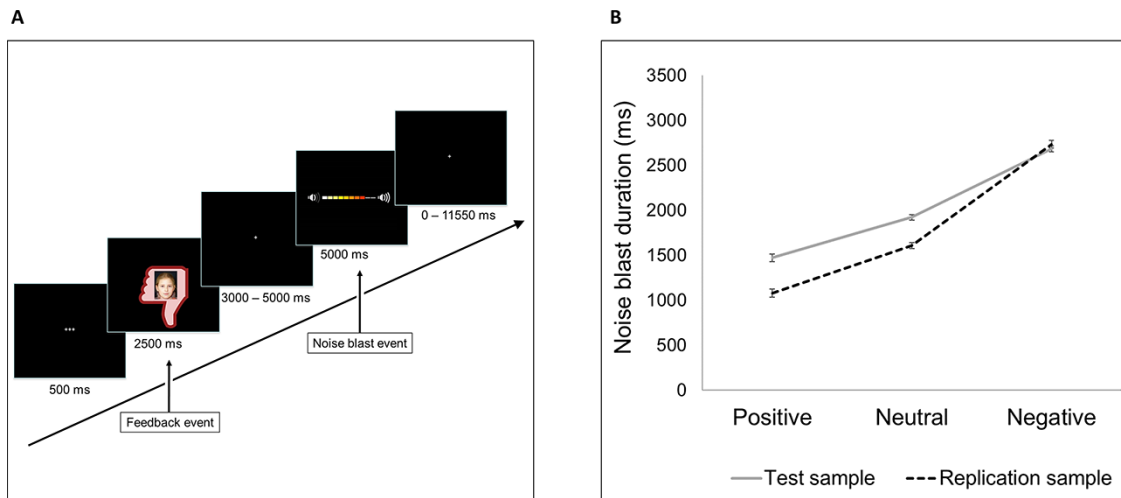
Fig. 1. SNAT. (A) Schematic representation of a trial with negative social feedback. (B) Noise blast duration for each feedback condition in the original sample (solid line) and replication sample (dotted line). Error bars represent standard errors.

of each participant were resampled to $3 \times 3 \times 3$ mm voxels. Data were spatially smoothed using a 6 mm full-width-at-half-maximum isotropic Gaussian kernel. For all participants, translational movement parameters were calculated. Participants were included in the first-level analysis when they had at least two runs of fMRI data with <3 mm maximum motion in every direction (x, y, z) (in line with the original study of Achterberg *et al.*, 2018). We included detailed information on motion parameters and small spikes (i.e. motion between 0.9 and 3 mm in any volume) in Supplementary Table S8. Most participants showed a limited number of small spikes [participants with small spikes in >10% of volumes in test sample: $n = 2$ (10.8% and 13.4%); in replication sample: $n = 4$ (12.4–19.0%); Supplementary Figure S4]. Moreover, the results did not differ between participants with small spikes and participants without small spikes (see sensitivity analyses in the Supplementary Results). Thus, we allowed this minimal amount of motion in order to weigh up against the possible extra loss of trials (Siegel *et al.*, 2014).

First-level analyses

We analyzed individual participant's data using a general linear model in SPM8. Two events were convolved with the hemodynamic response function (HRF) to model the fMRI time series. The onset of feedback delivery was modeled as the feedback event, with a zero duration and with valence of the feedback as separate regressors ('positive', 'neutral' and 'negative'). The start of the noise blast was modeled as the noise blast event, with the HRF modeled for the length of the noise blast duration and with noise blast following positive, neutral and negative feedback as separate regressors (Achterberg *et al.*, 2018; van de Groep *et al.*, 2021, 2022). Trials on which participants did not respond in time were marked as invalid and excluded from analysis. Six motion regressors were added to the model as covariates of no interest. We used the least-squares parameter estimates (PEs) of height of the best-fitting canonical HRF for each condition in pairwise contrasts. The resulting subject-specific contrast images were used in the group-level analyses.

Second-level analyses

To investigate feedback effects on neural responses during the social feedback event, we performed a full-factorial analysis of variance (ANOVA) with three levels (feedback: 'Positive', 'Neutral' and 'Negative') on data of the replication sample. The whole-brain analyses of the test sample were previously reported in Achterberg *et al.* (2018). We calculated the 'Negative > Positive' and 'Positive > Negative' contrasts and investigated activation that was specific to both positive and negative feedback (compared to neutral feedback) by performing a conjunction analysis (of the contrasts 'Negative > Neutral' and 'Positive > Neutral') with the 'logical AND' strategy. This strategy requires activation in both contrasts to be individually significant (Nichols *et al.*, 2005).

In addition, we investigated feedback effects on neural responses during the noise blast event by performing a full-factorial ANOVA with three levels (noise after feedback: 'PositiveNoise', 'NeutralNoise' and 'NegativeNoise'). These whole-brain analyses were conducted in both samples since they were not previously reported. We explored the following contrasts: 'PositiveNoise > NegativeNoise' (and vice versa), 'PositiveNoise > NeutralNoise' (and vice versa) and 'NegativeNoise > NeutralNoise' (and vice versa).

All results were family-wise error (FWE) cluster-level corrected ($P_{FWEcc} < 0.05$) with an initial voxel-wise threshold of $P < 0.005$ (uncorrected) (Achterberg *et al.*, 2020). We report coordinates for local maxima in MNI space. The results of the whole-brain analyses are reported in the Supplementary material. Untresholded statistical maps of the whole-brain contrasts are available on Neurovault (Gorgolewski *et al.*, 2015) via https://neurovault.org/collections/GMFZUABO/.

Region of interest analyses

For the social feedback event, we used the regions of interest (ROIs) that were previously used in Achterberg *et al.* (2020): bilateral AI, bilateral VLPFC, dorsal MPFC and left DLPFC. PEs (average beta values) for each participant in the replication sample were extracted from the contrasts 'Positive > Fixation', 'Neutral > Fixation' and 'Negative > Fixation'.

For the noise blast event, we based our ROIs on whole-brain activation in the test sample and used the same ROIs in our replication sample. In the test sample, clusters of activation from the whole-brain contrasts were extracted using SPM8's MarsBar toolbox (Brett *et al.*, 2002). Based on a priori hypotheses, we selected the following five regions: the

bilateral AI and bilateral VLPFC (from the 'AllNoise > Fixation' contrast), the bilateral MPFC and bilateral OFC (from the conjunction contrasts of 'NegativeNoise > NeutralNoise' and 'PositiveNoise > NeutralNoise') and the bilateral DLPFC (from the conjunction contrasts of 'PositiveNoise > NegativeNoise' and 'NeutralNoise > NegativeNoise'). These clusters of activation were masked with regions from the Automated Anatomical Labeling atlas (Tzourio-Mazoyer *et al.*, 2002) to construct our final ROIs (see https://osf.io/tc83e/ for the 3D NIfTI files). For both samples, PEs for each participant were extracted from the contrasts of 'PositiveNoise > Fixation', 'NeutralNoise > Fixation' and 'NegativeNoise > Fixation'.

Statistical analyses

Outliers were defined as Z-scores of <-3.29 or >3.29 on each variable, and these data points were excluded from subsequent analyses. No outliers were observed in the behavioral data. In the ROI data, maximally 2% of the data were defined as outliers.

Confirmatory analyses

Valence effects. To test the effects of feedback conditions on noise blast duration and ROI activation during feedback and noise blast, we used a linear mixed model approach in R (R Core Team, 2013) using the lme4 package (Bates *et al.*, 2015). Data were fitted on the average noise blast duration (for behavioral analyses) and the average PEs (for ROI analyses on the feedback and noise blast events) for each feedback condition (positive, neutral and negative). The use of linear mixed models allowed us to add two random factors to our model: ChildID to account for the nesting of feedback conditions within children and FamilyID to account for the nesting of children within families. Note that our participants were twins, who shared the same family environment within a twin pair. Feedback condition was added as a fixed effect (three levels: positive, neutral and negative) and sex as a covariate, including interaction effects with conditions. Thus, we defined our linear mixed model in R as follows: Noise blast duration/ROI ~ Condition × Sex + (1|ChildID) + (1|FamilyID). We inspected the results with type III ANOVA's using Satterthwaite's method. Significant main effects were *post hoc* inspected using least-square means with Kenward–Roger corrected degrees of freedom and Bonferroni-adjusted *P*-values (Achterberg *et al.*, 2020). In an additional analysis, we tested for valence effects on nucleus accumbens activation during noise blast (see Supplementary Results and Supplementary Figure S2).

In sensitivity analyses, we checked whether the addition of a random slope of condition on the family level changed the results. We defined this model in R as follows: ROI ~ Condition × Sex + (1|ChildID) + (1 + Condition|FamilyID) and checked whether the model fit increased compared to the original model, using log-likelihood tests with the anova function in R. For models on ROI activation during the feedback event, adding a random slope did not increase model fit (all $P > 0.05$). For models on ROI activation during the noise blast event, adding a random slope did increase the model fit (all $P < 0.05$). For this event, we report the results of the linear mixed models with a random slope in Supplementary Tables S6 and S7.

Since the L-CID study included a randomized controlled trial, ~40% of the families received an intervention to promote positive parenting and sensitive discipline (VIPP-SD; Euser *et al.*, 2016, 2021) between T2 and T3 (Crone *et al.*, 2020). As a sensitivity check, we repeated our replication analyses in the control group of the VIPP-SD. In an additional sensitivity analysis, we checked for possible intelligence quotient (IQ) effects by adding IQ as a covariate to the linear mixed models. In both analyses, the results did not meaningfully differ from the results described in the paper (Supplementary material).

Brain–behavior analyses. To test whether we could replicate the finding that increased DLPFC activation during feedback was related to shorter noise blasts following negative feedback, we used the DLPFC ROI from the whole-brain regression on the test sample reported in Achterberg *et al.* (2020). Using least-square regressions, we specifically tested whether DLPFC activation (PE) in this ROI during the feedback event ('Negative – Neutral') negatively predicted noise blast duration (Δ negative – neutral) in the independent replication sample.

For the noise blast event, we performed a whole-brain regression in the test sample ('PositiveNoise – NegativeNoise') with the difference in noise blast duration following positive and negative feedback as a regressor (Δ positive – negative). The results were FWE voxel-level corrected with $P_{FWE} < 0.05$. For our replication analysis, we tested whether DLPFC activation (PE) in this ROI during the noise blast event ('PositiveNoise – NegativeNoise') predicted noise blast duration (Δ positive – negative) in the replication sample. Activation in the left and right DLPFC was correlated, $r = 0.91$, $P < 0.001$, so we used the mean score in the replication analysis. Because twins are nested in families, the assumption of homoscedasticity is violated. To correct this violation, we used heteroscedasticity-consistent standard errors (HCSE) estimators (Hayes and Cai, 2007) in our regression analyses.

Equivalence testing. To investigate replication effects, we used equivalence testing in R (TOSTER package 0.3.4; Lakens, 2017) in addition to null-hypothesis significance testing for effects that we could not replicate. Equivalence testing tests whether the hypothesis that replication effects are large enough to be considered meaningful, i.e. the smallest effect size of interest (SESOI; Lakens *et al.*, 2018), is rejected. For our replication analyses, we defined the SESOI as the lower boundary of the confidence interval of the effect in the test sample (Perugini *et al.*, 2014; Lakens *et al.*, 2018).

Exploratory analyses

In exploratory analyses, we tested for age effects and for moderation effects by inhibitory control. For these analyses, we combined data from both samples to increase power.

Age effects. First, we tested for age effects on feedback processing and subsequent responses in middle childhood (behavioral: $n = 863$, MRI: $n = 580$). We added age (rounded to two decimal places, grand mean-centered) to our linear mixed models in R, including interaction effects of age and feedback condition. Because we combined two samples, we controlled for cohort (MCC or ECC) in our analyses. Thus, our linear mixed model in R was defined as follows: Noise blast duration/ROI ~ Condition × Age + Condition × Sex + Condition × Cohort + (1|ChildID) + (1|FamilyID). In sensitivity analyses, we added a random slope of condition on family level to the linear mixed model to check whether this increased model fit and changed the results. This linear mixed model in R was defined as follows: ROI ~ Condition × Age + Condition × Sex + Condition × Cohort + (1|ChildID) + (1 + Condition|FamilyID). Again, model fit increased only for linear mixed models on ROI activation during the noise blast event.
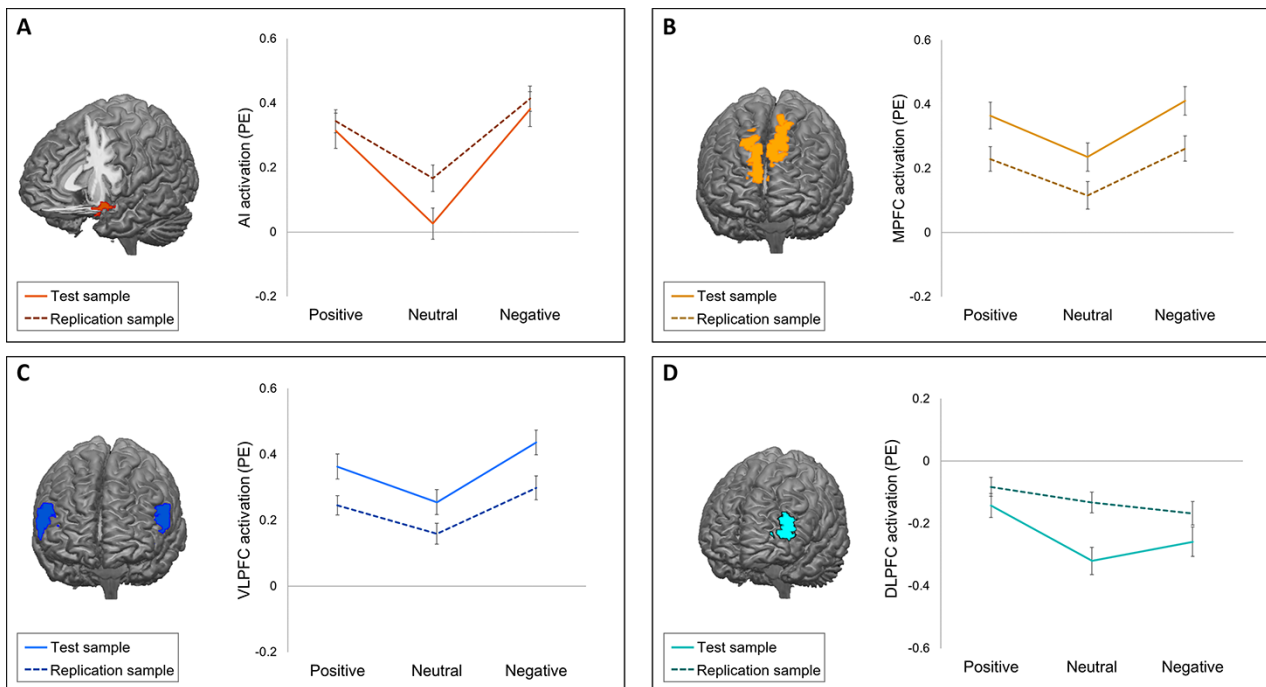
Fig. 2. Neural activation (PEs) during the feedback event for each feedback condition in four ROIs in the test sample (solid lines) and replication sample (dotted lines). Error bars represent standard errors. (A) Activation in the AI. (B) Activation in the MPFC. (C) Activation in the VLPFC. (D) Activation in the DLPFC.

Moderation inhibitory control. To test whether inhibitory control moderated the association between MPFC/AI activation during feedback and subsequent noise blast duration, we performed two moderation analyses ($n = 549$).

Moderation analyses were performed using the PROCESS macro (version 3.5) in R (Hayes, 2017). First, we performed a moderation analysis with AI activation during feedback ('Negative – Neutral') as an independent variable, noise blast duration (Δ negative – neutral) as a dependent variable and inhibitory control as a moderator. Next, we performed a second moderation analysis with MPFC activation during feedback ('Negative – Neutral') as an independent variable, noise blast duration (Δ negative – neutral) as a dependent variable and inhibitory control as a moderator. To control for sample effects, cohort (MCC or ECC) was added as a covariate in both analyses.

Results
Behavioral results
Valence effects
ECC replication sample. Replicating prior findings, we found a main effect of social feedback condition on noise blast duration, $F(2708) = 490.76$, $P < 0.001$ (Figure 1B). Mean noise blast duration was the longest following negative feedback, followed by shorter noise blasts following neutral and shortest following positive feedback (all pairwise comparisons, $P < 0.001$). Additionally, the model revealed a sex effect [$F(1179.86) = 9.55$, $P = 0.002$], indicating longer noise blast durations for boys than girls.

Neural activation during feedback
Valence effects
ECC replication sample. We replicated previously reported valence effects on neural activation during feedback (Figure 2;

Supplementary Tables S2 and S3). The differences that were found compared to the test sample were nonequivalent to zero (Supplementary material).

Brain–behavior analyses
ECC replication sample. We observed a significant negative correlation between noise blast duration following negative (*vs* neutral) feedback and DLPFC activation during negative feedback (*vs* neutral feedback), $r = -0.16$, $P = 0.023$ (HCSE-corrected; Figure 4A). This effect was specific to noise blast duration following negative *vs* neutral feedback and negative *vs* positive feedback, as no correlations were found between DLPFC activation and noise blast duration following positive, negative or neutral, or positive *vs* neutral feedback (Table 2).

Neural activation during noise blast
Noise blast neural activation has not been reported previously for any of the cohorts; therefore, we first report the results of the MCC test sample and then the results of the ECC replication sample.

Valence effects
MCC test sample. In all five ROIs of the noise blast event, we found a main effect of feedback condition on neural activation (Figure 3). However, patterns of activation differed between ROIs (see Supplementary Table S5 for *post hoc* test statistics). For the MPFC [$F(2752.55) = 13.75$, $P < 0.001$] and OFC [$F(2756.53) = 11.67$, $P < 0.001$], activation during the noise blast event was lower following neutral compared to negative feedback ($P \leq 0.01$) and lower following neutral compared to positive feedback ($P \leq 0.003$). For MPFC activity, we also observed an interaction effect of condition and sex, $F(2752.55) = 3.89$, $P = 0.02$, indicating stronger condition effects for girls than for boys. For

Table 2. Correlation analyses between DLPFC activation during feedback and subsequent noise blast duration in the test and replication sample

		Noise blast duration negative – neutral	Noise blast duration negative – positive	Noise blast duration negative	Noise blast duration positive – neutral	Noise blast duration positive	Noise blast duration neutral
DLPFC[a] replication sample	r	–0.16	–0.12	–0.02	–0.09	–0.11	–0.08
	P	0.023	0.032	0.809	0.179	0.119	0.354
DLPFC[a] test sample	r	–0.06	–0.09	0.00	–0.02	–0.01	0.01
	P	0.249	0.124	0.955	0.695	0.899	0.852

Note. P-values are corrected with HCSE estimates.
[a]DLPFC ROI from whole-brain regression (with the difference in noise blast duration negative – neutral as a regressor) of Achterberg *et al.* (2020).
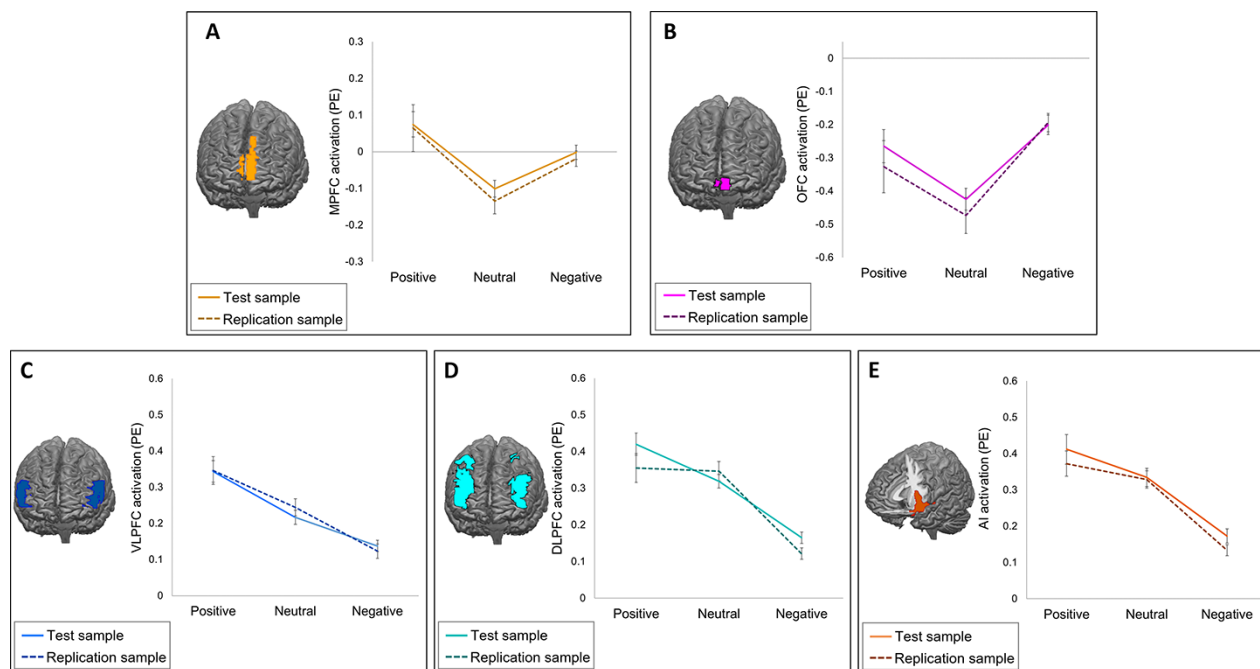

Fig. 3. Neural activation (PEs) during the noise blast event for each feedback condition in five ROIs in the test sample (solid lines) and replication sample (dotted lines). Error bars represent standard errors. (A) Activation in the MPFC. (B) Activation in the OFC. (C) Activation in the VLPFC. (D) Activation in the DLPFC. (E) Activation in the AI.

the DLPFC [$F(2757.79 = 43.83$, $P < 0.001$], VLPFC [$F(2745.60) = 29.73$, $P < 0.001$] and AI [$F(2748) = 22.89$, $P < 0.001$], activation following negative feedback was significantly lower than following neutral feedback (all $P \leq 0.01$) and positive feedback (all $P < 0.001$). For the DLPFC and VLPFC, but not AI, activation following neutral feedback was also lower compared to positive feedback (both $P < 0.001$).

ECC replication sample. We repeated the ROI analyses in the replication sample and found similar patterns of activation (Figure 3) in all five ROIS [MPFC: $F(2386.74) = 6.04$, $P = 0.003$; OFC: $F(2383.42) = 6.69$, $P = 0.001$; DLPFC: $F(2381.04) = 25.90$, $P < 0.001$; VLPFC: $F(2378.81) = 20.79$, $P < 0.001$; AI: $F(2381.45) = 29.14$, $P < 0.001$]. However, some differences were found compared to the original sample. For the MPFC, the difference between negative feedback and neutral feedback was no longer significant, $P = 0.181$. Equivalence testing against raw equivalence bounds of –0.01 and 0.01 revealed that this effect was statistically nonequivalent to zero, $t(191) = 3.03$, $P = 0.999$. For OFC activation, the difference between positive feedback and neutral feedback

was no longer significant, $P = 0.191$. Equivalence testing against equivalence bounds of –0.04 and 0.04 again revealed that this effect was nonequivalent to zero, $t(189) = 1.23$, $P = 0.890$. Finally, the difference between DLPFC activation in the positive and neutral feedback conditions was no longer significant, $P = 1$. Equivalence testing against equivalence bounds of –0.04 and 0.04 was nonsignificant, $t(189) = –0.76$, $P = 0.224$. *Post hoc* statistics are presented in Supplementary Table S5. The results were comparable using linear mixed models with a random slope of condition (Supplementary Tables S6 and S7).

Brain–behavior analyses
MCC test sample. A whole-brain regression analysis with noise blast duration (negative – positive) as a regressor resulted in increased activation in several areas, including the left and right DLPFC (Figure 4B). Specifically, we found a negative relation between DLPFC activation during the noise blast and noise blast duration. A *post hoc* correlation analysis showed that more DLPFC activation during the noise blast was associated with shorter noise blasts, $r = –0.45$, $P < 0.001$ (HCSE-corrected; Table 3).
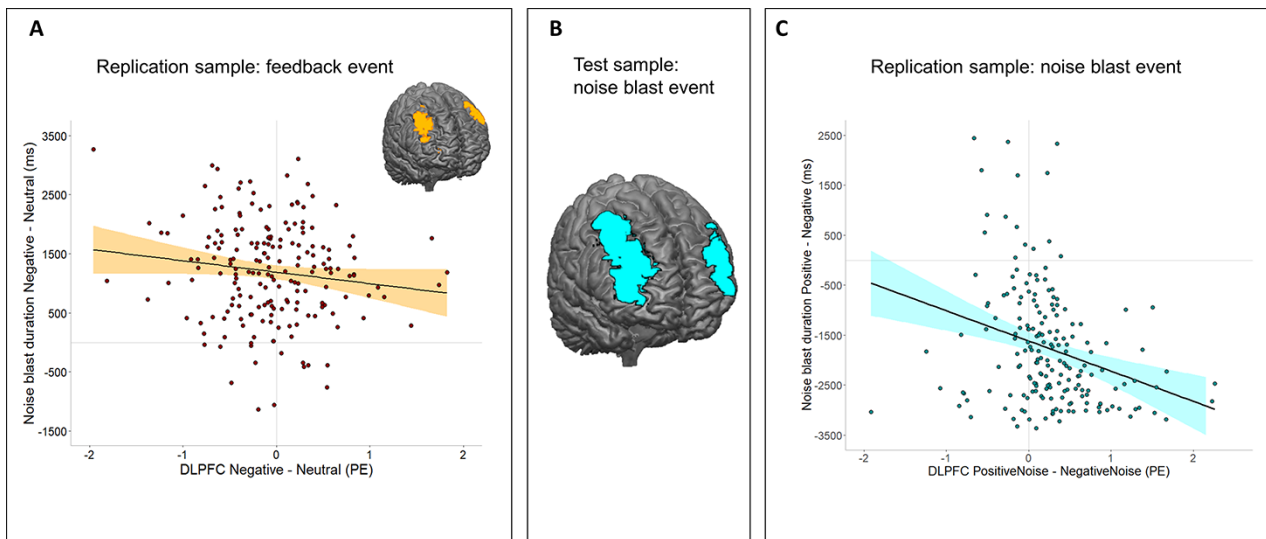
Fig. 4. Brain–behavior relations during the feedback and noise blast event. (A) Brain–behavior association during feedback in the replication sample. (B) Significant cluster of activation in the bilateral DLPFC in the test sample for the contrast PositiveNoise > NegativeNoise with noise blast (Δ positive – negative) as a regressor. (C) Brain–behavior association during noise blast in the replication sample.

Table 3. Correlation analyses between DLPFC activation during noise blast and noise blast duration in the test and replication sample

		Noise blast duration positive – negative	Noise blast duration negative – neutral	Noise blast duration negative	Noise blast duration positive – neutral	Noise blast duration positive	Noise blast duration neutral
DLPFC[a] replication sample	r	−0.31	−0.46	−0.51	−0.30	−0.23	−0.44
	P	<0.001	<0.001	<0.001	<0.001	0.001	<0.001
DLPFC[a] test sample	r	−0.45	−0.42	−0.37	−0.26	−0.37	−0.34
	P	<0.001	<0.001	<0.001	<0.001	<0.001	<0.001

Note. P-values are corrected with HCSE estimates.
[a]DLPFC ROI from whole-brain regression (with the difference in noise blast duration positive – negative as a regressor) in the original sample (MCC).

ECC replication sample. Using the DLPFC from the whole-brain regression in the test sample as ROI, we replicated the significant negative relation between noise blast duration (positive – negative) and activation in the DLPFC, $r = -0.31$, $P < 0.001$ (HCSE-corrected; Figure 4C). Additional correlation analyses, however, revealed that this DLPFC activation was also negatively related to noise blast duration following positive *vs* neutral and negative *vs* neutral feedback (all $P \leq 0.001$; Table 3).

Exploratory analyses
Age effects
We explored age-related effects, by testing the effects of age on the valence effects on noise blast duration and ROI activation. There was a significant main effect of age on noise blast duration, $F(1436.73) = 8.38$, $P = 0.004$, $\eta^2_p = 0.02$, indicating higher mean noise blast duration for younger children. The results also revealed an interaction effect between age and feedback condition, $F(21726) = 23.27$ $P < 0.001$, $\eta^2_p = 0.03$, such that noise blast duration following negative feedback increased and noise blast duration following positive feedback decreased with age (Figure 5A).

We did not find any age effects on DLPFC, VLPFC, MPFC and AI activation during feedback (all $P > 0.251$).

During the noise blast, the results revealed a main effect of age on activation in the DLPFC [$F(1325.03) = 12.33$, $P < 0.001$,

$\eta^2_p = 0.04$], VLPFC [$F(1305.54 = 10.28$, $P = 0.001$, $\eta^2_p = 0.03$], MPFC [$F(1297.98) = 4.38$, $P = 0.037$, $\eta^2_p = 0.01$] and AI [$F(1332.56) = 6.30$, $P = 0.012$, $\eta^2_p = 0.02$], indicating increased activation for older children. In four ROIs, there was a significant interaction between condition and age [DLPFC: $F(21137.65) = 11.02$, $P < 0.001$, $\eta^2_p = 0.02$; VLPFC: $F(21123) = 9.16$, $P < 0.001$, $\eta^2_p = 0.02$; MPFC: $F(21140.72) = 4.58$, $P = 0.010$, $\eta^2_p = 0.01$; AI: $F(21120.37) = 4.73$, $P = 0.009$, $\eta^2_p = 0.01$]. These interactions demonstrated that activation during aggression following positive feedback significantly increased with increasing age (all $P < 0.001$), whereas activation during aggression following negative and neutral feedback remained stable (all $P > 0.085$; Figure 5B). The results were comparable when using linear mixed models with a random slope of condition, with the exception that the main and interaction effects of the MPFC were no longer significant [main effect of age: $F(1328.57) = 3.75$, $P = 0.077$, $\eta^2_p = 0.01$; interaction effect: $F(2423.29) = 2.59$, $P = 0.076$, $\eta^2_p = 0.01$]. Thus, these results were less robust and should be interpreted with caution.

Moderation inhibitory control
To test whether inhibitory control moderated the relation between MPFC/AI activation and noise blast duration, we performed two moderation analyses. The results showed that there were no moderation effects of inhibitory control (Supplementary material). In sensitivity analyses, we checked whether the results
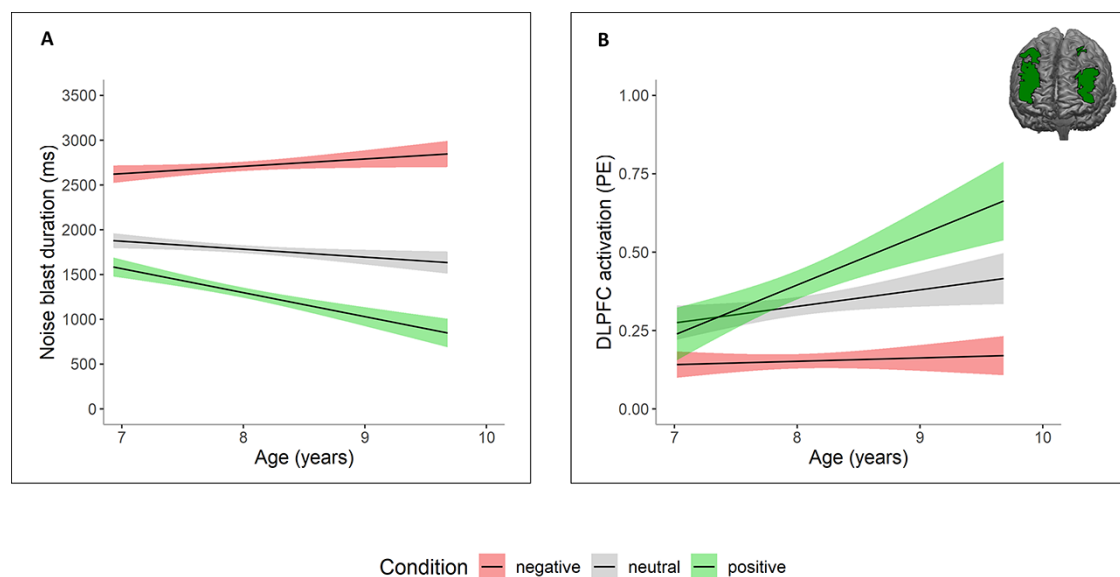
Fig. 5. Age effects for each feedback condition. (A) Age effects on noise blast duration: older children show more behavioral differentiation between feedback conditions. (B) Age effects on DLPFC activation during noise blast: older children show increased activation following positive feedback. Similar relations were found for MPFC, VLPFC and insula activation.

were similar using data of the Stop-Signal Task as a behavioral proxy of inhibitory control (Williams *et al.*, 1999). Again, we did not find moderation effects (Supplementary Results).

Discussion

This study examined the behavioral and neural mechanisms of feedback processing and subsequent aggressive responses in middle childhood, using a test-replication design. Specifically, our study answered three main questions. First, we replicated the behavioral and neural findings on feedback processing of Achterberg *et al.* (2020). Behaviorally, negative social feedback resulted in aggressive responses, which is a consistent finding in children (Achterberg *et al.*, 2017, 2018) and adults (Chester *et al.*, 2018). fMRI analyses revealed most activation in the AI and MPFC during positive and negative feedback and in the VLPFC during negative feedback, confirming prior work showing that these regions respond to socially salient events (Dalgleish *et al.*, 2017; Achterberg *et al.*, 2018) and rejection (Eisenberger *et al.*, 2003). Second, in two independent samples, we consistently found valence effects during responses to social feedback. The MPFC and OFC showed the most activation following positive and negative feedback, and the DLPFC, VLPFC and AI showed the least activation following negative feedback. Third, we observed brain–behavior relations during feedback and aggressive behavior: more DLPFC activation during negative feedback processing was related to less subsequent aggression, whereas more DLPFC activation during the noise blast event was generally related to less aggression (independent of the valence of the feedback). Age analyses revealed that older children showed less aggression in general and differentiated more in noise blasts following positive and negative feedback. Moreover, we found age effects in brain activation during the noise blast, but not during social feedback processing. That is, older children showed more neural activation during the noise blast following positive feedback. These findings indicate that responses to social feedback show developmental changes from middle to late childhood.

A novel question in this study was to examine the neural responses during responses to social feedback. Given that few studies incorporated a condition in which participants received positive feedback before being instructed to send a noise blast, it is interesting to note that in our study, sending noise blasts following positive feedback resulted in a wide network of activation, including the DLPFC, VLPFC and AI. These findings are in line with a recent study by van de Groep *et al.* (2021), who also reported increased activation in several regions including the lateral PFC when responding to positive compared to neutral and negative feedback. Possibly, responses to positive feedback might result in more cognitive control and intentional inhibition tendencies (Filevich *et al.*, 2012) compared to negative and neutral feedback, especially in the SNAT paradigm where participants were instructed to always send a noise blast. Indeed, noise blast duration was the shortest following positive feedback. Activation in lateral prefrontal regions, ACC and SMA has previously been linked to inhibitory control and executive functioning (Schel *et al.*, 2014; Crone and Steinbeis, 2017), and this network seems to be in place already in middle childhood (Engelhardt *et al.*, 2019). Prior studies showed that inhibition is a multi-dimensional construct (Ridderinkhof *et al.*, 2014) and theoretical reviews distinguished between stimulus-driven and intentional inhibition, which were associated with separable neural networks (Filevich *et al.*, 2012; Schel *et al.*, 2014). Possibly, the current paradigm relied most on intentional inhibition processes. Alternatively, however, activation in these regions following positive feedback could also be indicative of increased confusion when having to respond aggressively to positive feedback or a contradiction of feelings of fairness. Indeed, the insula and lateral prefrontal cortex were previously found to be involved in responding to conflicting information (Kim *et al.*, 2010; Zaki *et al.*, 2010) and in normative decision-making (Buckholtz, 2015; Feng *et al.*, 2015). Interestingly, in our study, the VLPFC and AI showed differential effects of feedback conditions during the feedback and noise blast events, which may suggest a flexible role in both signaling for social saliency (Dalgleish *et al.*, 2017) and emotion regulation following

threat (Zhao *et al.*, 2021), as well as in inhibitory processes (Nelson and Guyer, 2011; Swick *et al.*, 2011). However, we did not use the exact same ROIs during the feedback and noise blast events, and thus these comparisons should be interpreted with caution.

Additionally, we examined brain–behavior relations between aggression and DLPFC activation. First, we replicated the finding that more DLPFC activation during negative (*vs* neutral) feedback was related to less aggression (Achterberg *et al.*, 2020). This correlation was specific to DLPFC activation in the negative feedback condition, which could fit with studies on the role of the DLPFC in emotion regulation and reappraisal of negative events (Ochsner *et al.*, 2012; Silvers and Guassi Moreira, 2019). During the noise blast event, specificity analyses revealed that more DLPFC activation was related to less aggression in general. The DLPFC has been found to play an important role in response inhibition in nonsocial contexts, such as in no-go paradigms (Durston *et al.*, 2002; Blasi *et al.*, 2006), and our findings suggest a similar role for the DLPFC in inhibitory control in a social context. Together, these brain–behavior relations reveal a robust regulatory mechanism in middle childhood.

In line with the notion that middle childhood is characterized by a rapid development in cognitive control functioning (Zelazo and Carlson, 2012), we observed age effects on behavioral aggression and neural activation during the noise blast event. Behaviorally, older children were less aggressive and showed more differentiation in aggression following negative and positive feedback. On a neural level, effects were most pronounced in the positive feedback condition, such that older children showed more activation in the DLPFC, VLPFC, AI and MPFC when responding to positive feedback. Prior studies also revealed a decrease in aggression from middle to late childhood (Chen *et al.*, 2011), with the largest decreases in responses following positive feedback (Achterberg *et al.*, 2020). Sensitivity to social evaluation and the importance of social belonging increase in adolescence (Somerville, 2013), which might cause older children to more often refrain from forced aggression following positive feedback. On the other hand, inhibitory control functions are still developing during childhood, which might possibly explain why we found increases in neural activation during aggression following positive feedback, but not in neural activation during feedback itself. In an exploratory moderation analysis, we tested the interaction of these two processes in predicting aggressive outcomes. However, we did not find any moderating effects of inhibitory control on the relation between neural social sensitivity and subsequent aggression in childhood, as was previously reported in adults (Chester *et al.*, 2014). Possibly, these mechanisms work differently in childhood when executive functions are still rapidly developing. Given that cognitive control functions continue to develop and social sensitivity peaks in adolescence (Somerville, 2013), an interesting direction for future research would be to explore whether the interaction of these processes is predictive of aggression in adolescence (Lickley and Sebastian, 2018).

This is the first study investigating neural mechanisms of both social feedback evaluation and subsequent responses in middle childhood, using a well-validated experimental task (Achterberg *et al.*, 2016, 2017). By including two large independent samples, we investigated the robustness and replicability of these mechanisms in middle childhood, which is still a relatively understudied phase in terms of neural development. Previously, it has been indicated that neuroimaging results often include false-positive results (Eklund *et al.*, 2016), possibly because of power issues (Button *et al.*, 2013; Turner *et al.*, 2018). Also, Elliott *et al.* (2020)

showed that task-based fMRI often shows low test–retest reliability and may often not be suitable to test for individual differences in small samples. However, the large sample sizes in our study compensated for these issues and may have increased the chance of replicating meaningful brain–behavior relations.

There were some limitations that should be considered as well when interpreting the results. First, there were differences between the two samples, such as the date of testing (2015 *vs* 2019), the number of trials or possible familiarity effects with the study (in the replication sample), which may have contributed to differences in results between the samples, such as smaller condition effects on ROI activation in the replication sample. However, since one might not expect to exactly replicate prior findings, we used equivalence testing to test whether a result would have been meaningful in the original study (Lakens *et al.*, 2018). Indeed, all non-replicable effects in the replication sample were nonequivalent to zero and therefore still considered meaningful. Thus, by and large our study did not show non-replicability of the original results and revealed some robust behavioral and neural effects on a group level and in individual differences analyses. An interesting approach for future studies would be to use correspondence testing, in which difference tests and equivalence testing are combined into one framework (Steiner and Wong, 2018). Second, since participants were instructed to always send a noise blast, it is difficult to discover whether some children would rather have refrained from aggression or would have acted prosocially when receiving positive feedback. Children who show both self-protective as well as prosocial behaviors were previously found to show decreased externalizing behaviors over time (Dobbelaar *et al.*, 2021). To further disentangle these possible motives and relations to developmental outcomes, future studies might include both an aggressive and prosocial response option, such as a noise blast measure that can both be increased and decreased. In keeping with prior studies, we modeled the HRF of the noise blast event as the duration of the noise blast length (van de Groep *et al.*, 2021, 2022). Adding a prosocial response option could also help in overcoming the issue that noise blast events for the three feedback conditions were modeled with different noise blast durations and might help shed light on the specific function of the DLPFC when responding to social feedback. Another possibility to keep conditions comparable is to let participants select a specific intensity of the noise blast (e.g. Krämer *et al.*, 2007; Chester *et al.*, 2018). Third, in our exploratory analyses, we tested for age effects cross-sectionally on a relatively narrow age range. To fully investigate developmental processes, it is necessary to investigate changes in within-subject behavior longitudinally during a broader developmental period. The period from childhood to adolescence might be specifically important in the context of aggression regulation, given the changes in emotional reactivity and cognitive control (Somerville, 2013; Crone and Steinbeis, 2017; Yoon *et al.*, 2018; Achterberg *et al.*, 2020). However, our findings on a relatively small age range already revealed developmental effects on aggression regulation, confirming the importance of middle childhood in social cognitive development.

In conclusion, our results highlight the importance of the affective salience network and prefrontal regions in social feedback processing and subsequent responses in middle childhood. This phase is marked by an increase in social experiences, during which aggressive responses following peer rejection may lead to a negative spiral of even more peer rejection (Lansford *et al.*, 2010). Thus, it is a crucial period to learn to regulate aggressive impulses. Our findings point toward the DLPFC as a flexible regulatory mechanism in both emotion regulation and inhibitory

behavior. Although we note developmental effects in these processes, our results reveal a core neural basis for social evaluation and aggression already in middle childhood. Together, these findings aid to our understanding of why some children are more prone to aggression than others.

Conflict of interest

The authors declared that they had no conflict of interest with respect to their authorship or the publication of this article.

Data availability

Data, study material and analysis code are available on DataverseNL through 10.34894/ZMUCKL.

Supplementary data

Supplementary data are available at *SCAN* online.

References

Apps, M.A.J., Rushworth, M.F.S., Chang, S.W.C. (2016). The anterior cingulate gyrus and social cognition: tracking the motivation of others. *Neuron*, **90**(4), 692–707.

Bates, D., Mächler, M., Bolker, B., Walker, S. (2015). Fitting linear mixed-effects models using lme4. *Journal of Statistical Software*, **67**(1), 1–48.

Beyer, F., Münte, T.F., Göttlich, M., Krämer, U.M. (2015). Orbitofrontal cortex reactivity to angry facial expression in a social interaction correlates with aggressive behavior. *Cerebral Cortex*, **25**(9), 3057–63.

Blakemore, S.-J., Mills, K.L. (2014). Is adolescence a sensitive period for sociocultural processing? *Annual Review of Psychology*, **65**(1), 187–207.

Blasi, G., Goldberg, T.E., Weickert, T., *et al.* (2006). Brain regions underlying response inhibition and interference monitoring and suppression. *European Journal of Neuroscience*, **23**(6), 1658–64.

Brett, M., Anton, J.-L., Valabregue, R., Poline, J.-B. (2002). Region of interest analysis using an SPM toolbox. *8th International Conference on Functional Mapping of the Human Brain*, **16**(2), 497.

Buades-Rotger, M., Brunnlieb, C., Münte, T.F., Heldmann, M., Krämer, U.M. (2016). Winning is not enough: ventral striatum connectivity during physical aggression. *Brain Imaging and Behavior*, **10**(1), 105–14.

Buckholtz, J.W. (2015). Social norms, self-control, and the value of antisocial behavior. *Current Opinion in Behavioral Sciences*, **3**, 122–9.

Button, K.S., Ioannidis, J.P.A., Mokrysz, C., *et al.* (2013). Power failure: why small sample size undermines the reliability of neuroscience. *Nature Reviews Neuroscience*, **14**(5), 365–76.

Chen, L., Zhang, W.-X., Ji, L.-Q., Chen, G.-H., Wei, X., Chang, S.-M. (2011). Developmental trajectories and gender differences of aggression during middle and late childhood. *Acta Psychologica Sinica*, **43**(6), 629–38.

Chester, D.S., Eisenberger, N.I., Pond, R.S., Richman, S.B., Bushman, B.J., Dewall, C.N. (2014). The interactive effect of social pain and executive functioning on aggression: an fMRI experiment. *Social Cognitive and Affective Neuroscience*, **9**(5), 699–704.

Chester, D.S., Lynam, D.R., Milich, R., DeWall, C.N. (2018). Neural mechanisms of the rejection-aggression link. *Social Cognitive and Affective Neuroscience*, **13**(5), 501–12.

Chester, D.S., DeWall, C.N. (2016). The pleasure of revenge: retaliatory aggression arises from a neural imbalance toward reward. *Social Cognitive and Affective Neuroscience*, **11**(7), 1173–82.

Cocosco, C.A., Kollokian, V., Kwan, R.K.-S., Pike, G.B., Evans, A.C. (1997). BrainWeb: online interface to a 3D MRI simulated brain database. *NeuroImage*, **5**, 425.

Crone, E.A., Achterberg, M., Dobbelaar, S., *et al.* (2020). Neural and behavioral signatures of social evaluation and adaptation in childhood and adolescence: the Leiden Consortium on Individual Development (L-CID). *Developmental Cognitive Neuroscience*, **45**(June), 100805.

Crone, E.A., Steinbeis, N. (2017). Neural perspectives on cognitive control development during childhood and adolescence. *Trends in Cognitive Sciences*, **21**(3), 205–15.

Dalgleish, T., Walsh, N.D., Mobbs, D., *et al.* (2017). Social pain and social gain in the adolescent brain: a common neural circuitry underlying both positive and negative social evaluation. *Scientific Reports*, **7**(1), 42010.

Dambacher, F., Sack, A.T., Lobbestael, J., Arntz, A., Brugman, S., Schuhmann, T. (2015). Out of control: evidence for anterior insula involvement in motor impulsivity and reactive aggression. *Social Cognitive and Affective Neuroscience*, **10**(4), 508–16.

Achterberg, M., van Duijvenvoorde, A.C.K., Bakermans-Kranenburg, M.J., Crone, E.A. (2016). Control your anger! The neural basis of aggression regulation in response to negative social feedback. *Social Cognitive and Affective Neuroscience*, **11**(5), 712–20.

Achterberg, M., van Duijvenvoorde, A.C.K., van der Meulen, M., Euser, S., Bakermans-Kranenburg, M.J., Crone, E.A. (2017). The neural and behavioral correlates of social evaluation in childhood. *Developmental Cognitive Neuroscience*, **24**, 107–17.

Achterberg, M., van Duijvenvoorde, A.C.K., van der Meulen, M., Bakermans-Kranenburg, M.J., Crone, E.A. (2018). Heritability of aggression following social evaluation in middle childhood: an fMRI study. *Human Brain Mapping*, **39**(7), 2828–41.

Achterberg, M., van Duijvenvoorde, A.C.K., van IJzendoorn, M.H., Bakermans-Kranenburg, M.J., Crone, E.A. (2020). Longitudinal changes in DLPFC activation during childhood are related to decreased aggression following social rejection. *Proceedings of the National Academy of Sciences of the United States of America*, **117**(15), 8602–10.

Achterberg, M., van der Meulen, M. (2019). Genetic and environmental influences on MRI scan quantity and quality. *Developmental Cognitive Neuroscience*, **38**, 100667.

DeFries, J.C., Plomin, R., Fulker, D.W., editors. (1994). *Nature and Nurture During Middle Childhood*. Oxford: Blackwell Publishing, p. 368.

Dobbelaar, S., van Duijvenvoorde, A.C.K., Achterberg, M., van der Meulen, M., Crone, E.A. (2021). A bi-dimensional taxonomy of social responsivity in middle childhood: prosociality and reactive aggression predict externalizing behavior over time. *Frontiers in Psychology*, **11**, 3986.

Durston, S., Thomas, K.M., Yang, Y., Uluğ, A.M., Zimmerman, R.D., Casey, B.J. (2002). A neural basis for the development of inhibitory control. *Developmental Science*, **5**(4), F9–16.

Eisenberger, N.I., Lieberman, M.D., Williams, K.D. (2003). Does rejection hurt? An fMRI study of social exclusion. *Science*, **302**(5643), 290–2.

Eklund, A., Nichols, T.E., Knutsson, H. (2016). Cluster failure: why fMRI inferences for spatial extent have inflated false-positive rates. *Proceedings of the National Academy of Sciences*, **113**(28), 7900–5.

Elliott, M.L., Knodt, A.R., Ireland, D., *et al.* (2020). What is the test-retest reliability of common task-functional MRI measures? New empirical evidence and a meta-analysis. *Psychological Science*, **31**(7), 792–806.

Engelhardt, L.E., Harden, K.P., Tucker-Drob, E.M., Church, J.A. (2019). The neural architecture of executive functions is established by middle childhood. *NeuroImage*, **185**, 479–89.

Euser, S., Bakermans-Kranenburg, M.J., van den Bulk, B.G., *et al.* (2016). Efficacy of the Video-feedback Intervention to promote Positive Parenting and Sensitive Discipline in Twin Families (VIPP-Twins): study protocol for a randomized controlled trial. *BMC Psychology*, **4**(1), 33.

Euser, S., Vrijhof, C.I., Van den Bulk, B.G., Vermeulen, R., Bakermans-Kranenburg, M.J., van IJzendoorn, M.H. (2021). Video-feedback promotes sensitive limit-setting in parents of twin preschoolers: a randomized controlled trial. *BMC Psychology*, **9**(1), 46.

Euston, D.R., Gruber, A.J., McNaughton, B.L. (2012). The role of medial prefrontal cortex in memory and decision making. *Neuron*, **76**(6), 1057–70.

Feng, C., Luo, Y.-J., Krueger, F. (2015). Neural signatures of fairness-related normative decision making in the ultimatum game: a coordinate-based meta-analysis. *Human Brain Mapping*, **36**(2), 591–602.

Filevich, E., Kühn, S., Haggard, P. (2012). Intentional inhibition in human action: the power of 'no'. *Neuroscience and Biobehavioral Reviews*, **36**(4), 1107–18.

Gilam, G., Lin, T., Raz, G., *et al.* (2015). Neural substrates underlying the tendency to accept anger-infused ultimatum offers during dynamic social interactions. *NeuroImage*, **120**, 400–11.

Gorgolewski, K.J., Varoquaux, G., Rivera, G., *et al.* (2015). NeuroVault.org: a web-based repository for collecting and sharing unthresholded statistical maps of the human brain. *Frontiers in Neuroinformatics*, **9**(p), 8.

Gunther Moor, B., van Leijenhorst, L., Rombouts, S.A.R.B., Crone, E.A., van der Molen, M.W. (2010). Do you like me? Neural correlates of social evaluation and developmental trajectories. *Social Neuroscience*, **5**(5), 461–82.

Guyer, A.E., Choate, V.R., Pine, D.S., Nelson, E.E. (2012). Neural circuitry underlying affective response to peer feedback in adolescence. *Social Cognitive and Affective Neuroscience*, **7**(1), 81–92.

Hayes, A.F. (2017). *Introduction to Mediation, Moderation, and Conditional Process Analysis: A Regression-based Approach*. New York: Guilford Publications.

Hayes, A.F., Cai, L. (2007). Using heteroskedasticity-consistent standard error estimators in OLS regression: an introduction and software implementation. *Behavior Research Methods*, **39**(4), 709–22.

Kim, C., Chung, C., Kim, J. (2010). Multiple cognitive control mechanisms associated with the nature of conflict. *Neuroscience Letters*, **476**(3), 156–60.

Krämer, U.M., Jansma, H., Tempelmann, C., Münte, T.F. (2007). Tit-for-tat: the neural basis of reactive aggression. *NeuroImage*, **38**(1), 203–11.

Lakens, D. (2017). Equivalence tests: a practical primer for t tests, correlations, and meta-analyses. *Social Psychological and Personality Science*, **8**(4), 355–62.

Lakens, D., Scheel, A.M., Isager, P.M. (2018). Equivalence testing for psychological research: a tutorial. *Advances in Methods and Practices in Psychological Science*, **1**(2), 259–69.

Lansford, J.E., Malone, P.S., Dodge, K.A., Pettit, G.S., Bates, J.E. (2010). Developmental cascades of peer rejection, social information processing biases, and aggression during middle childhood. *Development and Psychopathology*, **22**(3), 593–602.

Lickley, R.A., Sebastian, C.L. (2018). The neural basis of reactive aggression and its development in adolescence. *Psychology, Crime & Law*, **24**(3), 313–33.

Lotze, M., Veit, R., Anders, S., Birbaumer, N. (2007). Evidence for a different role of the ventral and dorsal medial prefrontal cortex for social reactive aggression: an interactive fMRI study. *NeuroImage*, **34**(1), 470–8.

Mehta, P.H., Beer, J. (2010). Neural mechanisms of the testosterone–aggression relation: the role of orbitofrontal cortex. *Journal of Cognitive Neuroscience*, **22**(10), 2357–68.

Menon, V., Uddin, L.Q. (2010). Saliency, switching, attention and control: a network model of insula function. *Brain Structure & Function*, **214**(5), 655–67.

Nelson, E.E., Guyer, A.E. (2011). The development of the ventral prefrontal cortex and social flexibility. *Developmental Cognitive Neuroscience*, **1**(3), 233–45.

Nichols, T., Brett, M., Andersson, J., Wager, T., Poline, J.-B. (2005). Valid conjunction inference with the minimum statistic. *NeuroImage*, **25**(3), 653–60.

Ochsner, K.N., Silvers, J.A., Buhle, J.T. (2012). Functional imaging studies of emotion regulation: a synthetic review and evolving model of the cognitive control of emotion. *Annals of the New York Academy of Sciences*, **1251**(1), E1–24.

Open Science Collaboration. (2015). Estimating the reproducibility of psychological science. *Science*, **349**(6251), aac4716.

Perugini, M., Gallucci, M., Costantini, G. (2014). Safeguard power as a protection against imprecise power estimates. *Perspectives on Psychological Science*, **9**(3), 319–32.

R Core Team. (2013). R: a language and environment for statistical computing.

Repple, J., Pawliczek, C.M., Voss, B., *et al.* (2017). From provocation to aggression: the neural network. *BMC Neuroscience*, **18**(1), 1–9.

Ridderinkhof, K.R., van den Wildenberg, W.P.M., Brass, M. (2014). "Don't" versus "Won't": principles, mechanisms, and intention in action inhibition. *Neuropsychologia*, **65**, 255–62.

Riva, P., Romero Lauro, L.J., DeWall, C.N., Chester, D.S., Bushman, B.J. (2015). Reducing aggressive responses to social exclusion using transcranial direct current stimulation. *Social Cognitive and Affective Neuroscience*, **10**(3), 352–6.

Schel, M.A., Scheres, A., Crone, E.A. (2014). New perspectives on self-control development: highlighting the role of intentional inhibition. *Neuropsychologia*, **65**, 236–46.

Schmidt, S. (2016). Shall we really do it again? The powerful concept of replication is neglected in the social sciences. In: *Methodological Issues and Strategies in Clinical Research*, 4th edn. Washington DC: American Psychological Association, pp. 581–96.

Siegel, J.S., Power, J.D., Dubis, J.W., *et al.* (2014). Statistical improvements in functional magnetic resonance imaging analyses produced by censoring high-motion data points. *Human Brain Mapping*, **35**(5), 1981–96.

Silvers, J.A., Guassi Moreira, J.F. (2019). Capacity and tendency: a neuroscientific framework for the study of emotion regulation. *Neuroscience Letters*, **693**(January 2017), 35–9.

Simonds, J., Kieras, J.E., Rueda, M.R., Rothbart, M.K. (2007). Effortful control, executive attention, and emotional regulation in 7–10-year-old children. *Cognitive Development*, **22**(4), 474–88.

Somerville, L.H. (2013). The teenage brain: sensitivity to social evaluation. *Current Directions in Psychological Science*, **22**(2), 121–7.

Steiner, P.M., Wong, V.C. (2018). Assessing correspondence between experimental and nonexperimental estimates in within-study comparisons. *Evaluation Review*, **42**(2), 214–47.

Swick, D., Ashley, V., Turken, U. (2011). Are the neural correlates of stopping and not going identical? Quantitative meta-analysis of two response inhibition tasks. *NeuroImage*, **56**(3), 1655–65.

Turner, B.O., Paul, E.J., Miller, M.B., Barbey, A.K. (2018). Small sample sizes reduce the replicability of task-based fMRI studies. *Communications Biology*, **1**(1), 62.

Tzourio-Mazoyer, N., Landeau, B., Papathanassiou, D., *et al.* (2002). Automated anatomical labeling of activations in SPM using a macroscopic anatomical parcellation of the MNI MRI single-subject brain. *NeuroImage*, **15**(1), 273–89.

van de Groep, I.H., Bos, M.G.N., Jansen, L.M.C., Achterberg, M., Popma, A., Crone, E.A. (2021). Overlapping and distinct neural correlates of self-evaluations and self-regulation from the perspective of self and others. *Neuropsychologia*, **161**, 108000.

van de Groep, I.H., Bos, M.G.N., Jansen, L.M.C., *et al.* (2022). Resisting aggression in social contexts: the influence of life-course persistent antisocial behavior on behavioral and neural responses to social feedback. *NeuroImage: Clinical*, **34**, 102973.

van IJzendoorn, M.H., Bakermans-Kranenburg, M.J. (2021). Replication crisis lost in translation? On translational caution and premature applications of attachment theory. *Attachment & Human Development*, **23**(4), 422–37.

White, S.F., Brislin, S.J., Sinclair, S., Blair, J.R. (2014). Punishing unfairness: rewarding or the organization of a reactively aggressive response? *Human Brain Mapping*, **35**(5), 2137–47.

Williams, B.R., Ponesse, J.S., Schachar, R.J., Logan, G.D., Tannock, R. (1999). Development of inhibitory control across the life span. *Developmental Psychology*, **35**(1), 205.

Yoon, L., Somerville, L.H., Kim, H. (2018). Development of MPFC function mediates shifts in self-protective behavior provoked by social feedback. *Nature Communications*, **9**(1), 3086.

Zaki, J., Hennigan, K., Weber, J., Ochsner, K.N. (2010). Social cognitive conflict resolution: contributions of domain-general and domain-specific neural systems. *The Journal of Neuroscience*, **30**(25), 8481.

Zelazo, P.D., Carlson, S.M. (2012). Hot and cool executive function in childhood and adolescence: development and plasticity. *Child Development Perspectives*, **6**(4), 354–60.

Zhao, J., Mo, L., Bi, R., *et al.* (2021). The VLPFC versus the DLPFC in downregulating social pain using reappraisal and distraction strategies. *Journal of Neuroscience*, **41**(6), 1331–9.